Real-time coherence imaging of suspicious breast masses recommended for aspiration or biopsy

Arunima Sharma[1], Eduardo A. Gonzalez[2], Emily Ambinder[3], Kelly Myers[3], Eniola Oluyemi[3], Muyinatu A. Lediju Bell[1,2,4,5]

[1]Department of Electrical and Computer Engineering, Johns Hopkins University, Baltimore, MD
[2]Department of Biomedical Engineering, Johns Hopkins University, Baltimore, MD
[3]Department of Radiology and Radiological Science, Johns Hopkins Medicine, Baltimore, MD
[4]Department of Computer Science, Johns Hopkins University, Baltimore, MD
[5]Department of Oncology, Johns Hopkins Medicine, Baltimore, MD

2023 IEEE International Ultrasonics Symposium (IUS) | 979-8-3503-4645-9/23/$31.00 ©2023 IEEE | DOI: 10.1109/IUS51837.2023.10307040

***Abstract*—Our group previously demonstrated that coherence-based imaging improves the certainty of fluid mass content in breast ultrasound images, and therefore has the potential to decrease unnecessary biopsies. However, this potential was demonstrated with post-processed raw channel data after patient examination. This work is the first to implement real-time short-lag spatial coherence (SLSC) imaging on an FDA-approved clinical ultrasound scanner to investigate a combined B-mode and coherence-based imaging approach to improve the diagnostic capabilities of breast ultrasound imaging. Real-time SLSC imaging was provided through GPU-based SLSC scripts that we developed and installed on our FDA-approved Alpinion ECUBE12R ultrasound scanner. A total of 47 hypoechoic breast masses from 32 patients were examined. First, the board-certified breast radiologists performing the patient exam predicted the mass contents and the BI-RADS category of the mass using real-time clinical B-mode images provided by the scanner. Then, the scanner was switched to present real-time SLSC images of the masses alongside real-time B-mode images, and the radiologist performing the scan repeated the predictions. The inclusion of SLSC images resulted in correct predictions of 100% of complicated cysts as BI-RADS 2 lesions (compared to 50% of complicated cysts being predicted as BI-RADS 2 lesions with only B-mode images). In addition, SLSC correctly identified presence of non-solid content in clusters of cysts, and no change in the BI-RADS category of malignant masses was observed after the inclusion of SLSC imaging. These results demonstrate the real-time potential of SLSC to decrease unnecessary biopsies by correctly identifying complicated cysts as benign fluid lesions.**

***Index Terms*—ultrasound, coherence beamforming, real-time, breast imaging**

I. Introduction

Breast cancer is the most common type of cancer among women in the United States, with approximately 12% of women diagnosed with the disease during their lifetimes [1]. Early diagnosis of breast cancer leads to good prognosis and high survival rate [1], [2]. Breast ultrasound is low-cost, ionizing radiation-free, and provides images in real-time. Therefore, it is widely used as a supplement to mammography during breast cancer screening and as the primary imaging modality during breast cancer diagnosis. However, the use of ultrasound imaging is limited due to its high false positive rate. Only 7-8% of breast biopsies performed under ultrasound guidance are found to yield cancer, demonstrating a large number of unnecessary biopsies or follow-up procedures [2], [3]. One reason for these high false positive rates is the presence of acoustic clutter in typical B-mode ultrasound images, which is due to multiple acoustic interactions between different layers of tissue [4], [5]. The presence of acoustic clutter leads to similar a hypoechoic appearance among some fluid-filled cysts and solid masses, resulting in diagnostic uncertainty.

Our group previously demonstrated that coherence-based beamforming, particularly short-lag spatial coherence (SLSC) beamforming [6] and Robust SLSC (R-SLSC) beamforming [7], reduces acoustic clutter and improves solid from fluid mass distinction [8], [9]. In addition, a retrospective reader study conducted with five board-certified breast radiologists demonstrated that the inclusion of coherence-based beamforming with B-mode imaging improved sensitivity of fluid-mass detection to 86% compared to 57% with B-mode alone and therefore, had a potential to reduce unnecessary biopsies to 13.3% from 43.3% [10], [11]. However, the studies were conducted outside the examination room (i.e., radiofrequency data acquired during patient examination were processed offline and the obtained images were collectively presented to the radiologists at a later date). This paper presents our initial results assessing the ability of real-time SLSC imaging to increase diagnostic certainty of fluid mass detection and decrease unnecessary biopsies during patient examination.

II. Methods

Thirty two patients scheduled for ultrasound-guided aspiration or core needle biopsy of at least one breast mass were enrolled in our study after receiving informed consent and approval from the Johns Hopkins Medicine Institutional Review Board (Protocol No. IRB00127110). Forty seven hypoechoic masses consisting of 8 fluid (4 simple cysts and 4 complicated cysts), 10 mixed (5 clusters of cysts, 1 epidermal inclusion cyst, and 4 complex solid and cystic), and 29 solid (18 benign, 1 high risk, and 10 malignant) masses were scanned using an Alpinion ECUBE12R research ultrasound scanner (Alpinion, Seoul, Korea). This scanner was connected to an Alpinion L8-17 probe with a center frequency of 12.5 MHz and a sampling frequency of 40 MHz. Simple cysts were classified as cysts without aspiration or biopsy because of clinical B-mode ultrasound features matching a simple cyst. Aspiration

was performed on masses that appeared fluid in nature, and the masses that were successfully aspirated were designated as complicated cysts. For the remaining masses, the pathology results of each core-needle biopsy served as the ground truth for mass classification.

The real-time reader study was similar to a retrospective reader study conducted previously [10], with the exception that this study was conducted during patient examination. After receiving informed consent from the study participants, our board-certified breast radiologist co-authors (E.O., K.M., or E.A.) performed the ultrasound scan. First, two orthogonal B-mode images of the mass were obtained using the in-built system beamformer. Based on the B-mode images, the radiologist performed two consecutive tasks: (1) classify the content of the mass (i.e., solid, fluid, mixed, or uncertain) and (2) provide a clinical diagnosis (i.e., the BI-RADS category for each mass [12]). Following classification with only real-time clinical-grade B-mode images, the scanner was switched to real-time SLSC mode and the same radiologist scanned the mass again to obtain similar orthogonal views. After visualizing the SLSC images, the radiologist performed the same two tasks. For each mass, screenshots and raw channel data were saved for comparative offline analyses.

SLSC imaging generally relies on the spatial coherence of delayed backscattered echoes received across the transducer aperture [6], [13]. Spatial coherence, $\hat{R}$, was calculated by normalizing the spatial covariance between equally spaced elements or lags by the variance of each time-delayed signal:

$$\hat{R}(m) = \frac{1}{N-m} \sum_{i=1}^{N-m} \frac{\sum_k s_{k,i}(n) s_{k,i+m}(n)}{\sqrt{\sum_k s_{k,i}^2(n) \sum_k s_{k,i+m}^2(n)}} \quad (1)$$

where m is the spatial lag (expressed as the number of element separations), N is the number of elements in the transducer, $s_i(n)$ is the time-delayed, zero-mean signal received at element i from depth n. These pixels are generated at each lateral and axial position with an axial correlation kernel, k, spanning depths n_1 to n_2. The value of the SLSC pixel was generated by summing the resulting spatial coherence function up to a specific short-lag value, M:

$$R_{sl} = \int_1^M \hat{R}(m) dm \approx \sum_{m=1}^{M} \hat{R}[m] \quad (2)$$

Real-time SLSC images were obtained by manipulating Eqs. (1)-(2) to fully utilize the benefits of the graphical processing unit (GPU) embedded in the ultrasound system. In particular, GPU-based SLSC scripts were developed using the same computations as those developed to obtain real-time photoacoustic SLSC images [14]–[16] and visualize SLSC images on the ultrasound scanner during the patient exam.

In contrast to the original SLSC implementation, which computes an average over an axial kernel to compute the cross-correlation (i.e., k in Eq. 1), the GPU SLSC implementation first computes individual correlation ($C_{i,j}$) and autocorrelation ($C_{i,i}$ and $C_{j,j}$) terms for scanline x, axial sample z, and elements i and j separated by m, given by the following equations:

$$C_{i,j}(z,x,m) = \sum_{i=1}^{N_i-m} s_i(z,x) s_{i+m}(z,x)^*, \quad (3)$$

$$C_{i,i}(z,x,m) = \sum_{i=1}^{N_i-m} |s_i(z,x)|^2, \quad (4)$$

$$C_{j,j}(z,x,m) = \sum_{i=1}^{N_i-m} |s_{i+m}(z,x)|^2, \quad (5)$$

where * denotes the complex conjugate. $C_{i,j}$, $C_{i,i}$, and $C_{j,j}$ were stored in the device global memory and then compounded across k, up to M, as follows:

$$SLSC(z,x) = \sum_{m=1}^{M} \frac{\sum_{\hat{z}\in k} C_{i,j}(\hat{z},x,m)}{\sqrt{\sum_{\hat{z}\in k} C_{i,i}(\hat{z},x,m) \sum_{\hat{z}\in k} C_{j,j}(\hat{z},x,m)}} \quad (6)$$

To create comparative offline and real-time SLSC images, Eq. (2) and Eq. (6), respectively, were computed for each lateral and axial pixel position with $k = 11$ and $M = 7$. All negative SLSC pixels were set to zero, and the images were log compressed and displayed with 60 dB dynamic range.

III. Results & Discussion

Fig. 1 shows screenshots of real time B-mode and SLSC images, and post processed B-mode and SLSC images example breast masses, which are visible as hypoechoic masses in both real-time and offline B-mode images. The spatial coherence of fluid-filled (i.e., complicated cyst) and mixed (i.e, cluster of cyst) masses is lower than that of the surrounding tissue, resulting in a darker appearance of the masses relative to the surrounding tissue in both real-time and offline SLSC images. In contrast, the spatial coherence of the benign and malignant solid masses are similar to that of the background tissue, resulting in these masses blending with the background in both real-time and offline SLSC images. Differences in signal amplitude, clutter levels, and image texture are observed between real-time and corresponding offline images, which can be attributed to proprietary, in-built, non-linear filters applied to the displayed images. Variations in traditional SLSC and GPU SLSC beamformers may also be partially responsible for the differences. However, similar to offline SLSC images, real-time SLSC images have the potential to differentiate solid from fluid masses.

Fig. 2 summarizes the radiologist classifications of complicated cysts, cluster of cysts, benign solid masses, and malignant solid masses (i.e., fluid or solid mass content and BI-RADS category). These classifications remained the same before and after including SLSC images when imaging simple cysts, an epidermal inclusion cyst, other mixed masses, and a high risk mass. Therefore, the results of these masses are not shown.

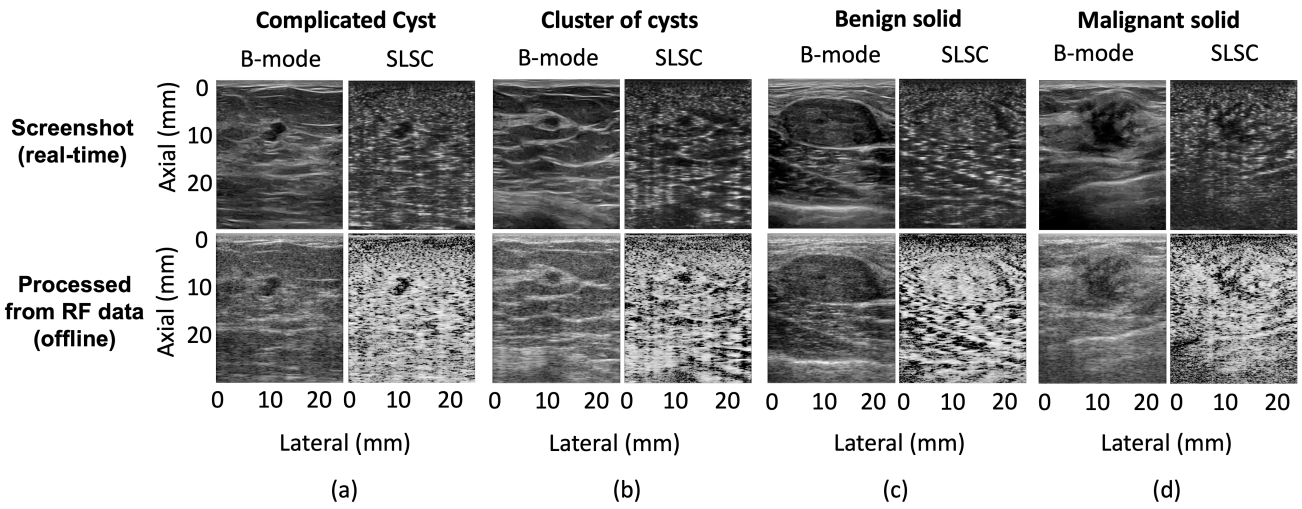

Fig. 1. Real time (top-row) and offline (bottom row) B-mode and SLSC images of an example each of (a) complicated cyst, (b) cluster of cysts, (c) benign solid mass, and (d) malignant solid mass. All images are displayed with 60dB dynamic range.

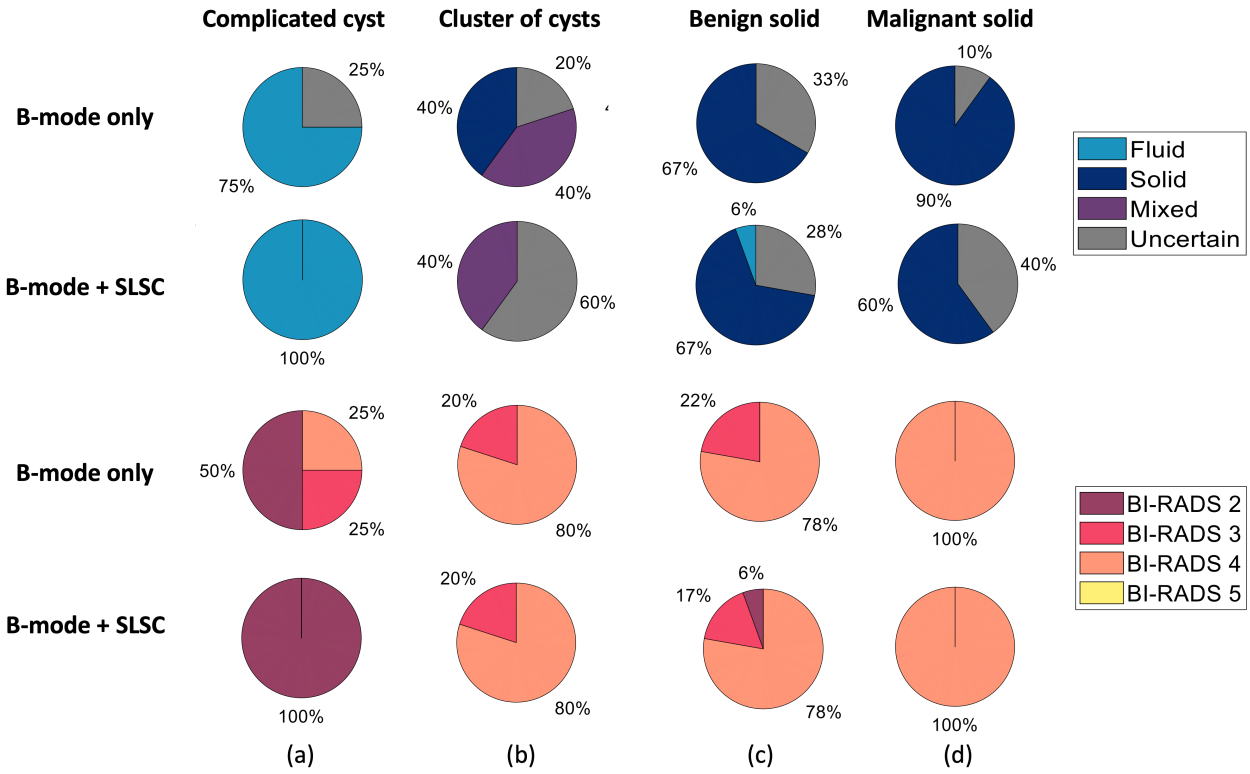

Fig. 2. Pie charts summarizing the results for classifying the mass contents (first and second rows) and BI-RADS categories (third and fourth rows) for (a) complicated cysts, (b) cluster of cysts, (c) benign solid masses, and (d) malignant solid masses with only B-mode imaging (first and third rows) and after inclusion of SLSC imaging (second and fourth rows) in real-time.

For complicated cysts (Fig. 2 (a)), the certainty of fluid content increased from 75% with B-mode images (first row) to 100% with SLSC images included (second row). In addition, with only B-mode images, 50% of complicated cysts were correctly categorized as benign masses (i.e., BI-RADS-2), 25% were recommended for follow-up (i.e., BI-RADS-3), and 25% were classified as suspicious masses recommended for biopsy (i.e., BI-RADS-4), as shown in the third row of Fig. 2 (a). With

the inclusion of SLSC images, 100% of complicated cysts were correctly identified as benign masses (i.e., BI-RADS-2), as shown in the fourth row of Fig. 2 (a). With complicated cysts being one of the most challenging masses to diagnose, these real-time results are promising to decrease the number of complicated cysts recommended for follow-up or biopsy when SLSC imaging is included in the diagnostic decision process.

Among the five clusters of cysts (Fig. 2(b)), two (40%) were classified as solid masses based on B-mode images, while the inclusion of SLSC images resulted in detecting presence of non-solid components in mixed masses. This change highlights the potential of SLSC to correctly identify that clusters of cysts are not purely solid masses. Otherwise, the BI-RADS classification of the clusters of cysts remained the same when comparing decisions based on B-mode alone (third row) to decisions made with the inclusion of SLSC (fourth row).

For the 19 benign solid masses (Fig. 2(c)), inclusion of SLSC imaging resulted in misclassification of one of the benign solid masses (6%) as a fluid mass. However, this mass was correctly classified as a benign BI-RADS category 2 mass after the SLSC inclusion. This result suggests the possibility of SLSC imaging to identify a subset of benign solid masses as benign masses, although additional investigation is required to identify this potential.

For the ten malignant solid masses (Fig. 2(d)), although the solid vs. fluid uncertainty increased with the inclusion of SLSC imaging, the BI-RADS classification rightfully remained the same with B-mode alone and after the inclusion of SLSC imaging (i.e., all of the malignant solid masses were recommended for biopsy).

The initial results of our real-time assessments confirm the potential of real-time SLSC imaging to identify fluid contents in breast masses and thereby prevent unnecessary biopsies of complicated cysts. In addition, the absence of a change in recommendations to biopsy the malignant masses after the inclusion of real-time SLSC imaging further supports the promise of this technique, as none of the malignant masses were misclassified as benign with the inclusion of SLSC imaging, which is critical for breast cancer detection.

IV. Conclusion

This work presents initial results demonstrating the application of real-time SLSC imaging to distinguish solid from fluid mass contents during ultrasound-based breast cancer diagnoses. The inclusion of real-time SLSC images improved the certainty of fluid mass contents in four complicated cysts from 75% with B-mode alone to 100% with the inclusion of SLSC images. In addition, the number of complicated cysts recommended for additional follow-up or biopsy was reduced from 50% with B-mode alone to 0% after the inclusion of SLSC images. These benefits were achieved without affecting the clinical conclusions for the malignant solid masses, which were all rightfully recommended for biopsy. These results provide promising support to include real-time SLSC images in clinical ultrasound scanners as a supplement to standard B-mode images to decrease the number of unnecessary biopsies and thereby decrease the false positive rate of breast ultrasound imaging.

Acknowledgment

This work is supported by NIH R01 EB032960.

References

[1] R. L. Siegel, K. D. Miller, N. S. Wagle, and A. Jemal, "Cancer statistics, 2023," *CA: A Cancer Journal for Clinicians*, vol. 73, no. 1, pp. 17–48, 2023.

[2] W. A. Berg, A. I. Bandos, E. B. Mendelson, D. Lehrer, R. A. Jong, and E. D. Pisano, "Ultrasound as the primary screening test for breast cancer: analysis from ACRIN 6666," *JNCI: Journal of the National Cancer Institute*, vol. 108, no. 4, 2016.

[3] W. A. Berg, Z. Zhang, D. Lehrer, R. A. Jong, E. D. Pisano, R. G. Barr, M. Böhm-Vélez, M. C. Mahoney, W. P. Evans, L. H. Larsen, M. J. Morton, E. B. Mendelson, D. M. Farria, J. B. Cormack, H. S. Marques, A. Adams, N. M. Yeh, G. Gabrielli, and f. t. ACRIN 6666 Investigators, "Detection of Breast Cancer With Addition of Annual Screening Ultrasound or a Single Screening MRI to Mammography in Women With Elevated Breast Cancer Risk," *JAMA*, vol. 307, no. 13, pp. 1394–1404, 04 2012.

[4] S. Huber, M. Wagner, M. Medl, and H. Czembirek, "Real-time spatial compound imaging in breast ultrasound," *Ultrasound in Medicine & Biology*, vol. 28, no. 2, pp. 155–163, 2002.

[5] M. A. Lediju, M. J. Pihl, J. J. Dahl, and G. E. Trahey, "Quantitative assessment of the magnitude, impact and spatial extent of ultrasonic clutter," *Ultrasonic Imaging*, vol. 30, no. 3, pp. 151–168, 2008.

[6] M. A. Lediju, G. E. Trahey, B. C. Byram, and J. J. Dahl, "Short-lag spatial coherence of backscattered echoes: Imaging characteristics," *IEEE Transactions on Ultrasonics, Ferroelectrics, and Frequency Control*, vol. 58, no. 7, pp. 1377–1388, 2011.

[7] A. A. Nair, T. D. Tran, and M. A. L. Bell, "Robust short-lag spatial coherence imaging," *IEEE Transactions on Ultrasonics, Ferroelectrics, and Frequency Control*, 2018.

[8] A. Wiacek, O. M. H. Rindal, E. Falomo, K. Myers, K. Fabrega-Foster, S. Harvey, and M. A. L. Bell, "Robust short-lag spatial coherence imaging of breast ultrasound data: Initial clinical results," *IEEE Transactions on Ultrasonics, Ferroelectrics, and Frequency Control*, vol. 66, no. 3, pp. 527–540, 2019.

[9] A. Wiacek, E. Falomo, K. Myers, O. M. H. Rindal, K. Fabrega-Foster, S. Harvey, and M. A. L. Bell, "Clinical feasibility of coherence-based beamforming to distinguish solid from fluid hypoechoic breast masses," in *2018 IEEE International Ultrasonics Symposium (IUS)*. IEEE, 2018, pp. 1–4.

[10] A. Wiacek, E. Oluyemi, K. Myers, L. Mullen, and M. A. L. Bell, "Coherence-based beamforming increases the diagnostic certainty of distinguishing fluid from solid masses in breast ultrasound exams," *Ultrasound in Medicine & Biology*, vol. 46, no. 6, pp. 1380–1394, 2020.

[11] ——, "Coherence-based beamforming improves the diagnostic certainty of breast ultrasound exams," in *2020 IEEE International Ultrasonics Symposium (IUS)*. IEEE, 2020, pp. 1–4.

[12] E. B. Mendelson, W. A. Berg, and C. R. Merritt, "Toward a standardized breast ultrasound lexicon, bi-rads: Ultrasound," *Seminars in Roentgenology*, vol. 36, no. 3, pp. 217–225, 2001, breast Imaging.

[13] M. A. L. Bell, J. J. Dahl, and G. E. Trahey, "Resolution and brightness characteristics of short-lag spatial coherence (SLSC) images," *IEEE Transactions on Ultrasonics, Ferroelectrics, and Frequency Control*, vol. 62, no. 7, pp. 1265–1276, 2015.

[14] E. Gonzalez, M. R. Gubbi, and M. A. L. Bell, "GPU implementation of coherence-based photoacoustic beamforming for autonomous visual servoing," in *Proceedings of the IEEE International Ultrasonics Symposium (IUS)*. IEEE, 2019, pp. 24–27.

[15] E. A. González and M. A. L. Bell, "GPU implementation of photoacoustic short-lag spatial coherence imaging for improved image-guided interventions," *Journal of Biomedical Optics*, vol. 25, no. 7, p. 077002, 2020.

[16] E. Gonzalez and M. A. L. Bell, "A gpu approach to real-time coherence-based photoacoustic imaging and its application to photoacoustic visual servoing," in *Photons Plus Ultrasound: Imaging and Sensing*, vol. 11240. SPIE, 2020, pp. 312–316.